EUROPEAN FUSION DEVELOPMENT AGREEMENT

EFDA–JET–CP(02)02-19

C. Fourment et al

Drift Wave Stability of ITB Reversed Magnetic Shear Discharges in JET

Drift Wave Stability of ITB Reversed Magnetic Shear Discharges in JET

C. Fourment, L.-G. Eriksson, X. Garbet, G.T. Hoang, X. Litaudon, G. Tresset,
and contributors to the EFDA-JET workprogramme*

Association EURATOM-CEA, DRFC, CEA Cadarache, 13108 St. Paul-lez-Durance, France
**See appendix of J. Paméla, Proc. 18th IAEA Conference on Fusion Energy, Sorrento 2000*

Preprint of Paper to be submitted for publication in
Proceedings of the 29th EPS Conference, (Montreux, Switzerland 17-21 June 2002)

I. INTRODUCTION

The role of the safety factor (q) and magnetic shear (s) in the formation of Internal Transport Barriers (ITBs) has been shown to be important in several tokamaks [1-5]. Recently JET experiments have been dedicated to the control of ITBs by optimizing the current profile [6]. This paper presents a comprehensive analyses of drift wave stability of JET plasmas with magnetic shear reversal. In the discharges analyzed, LHCD was applied to form a hollow current profile. The stability analysis has been carried out with the linear gyrokinetic code KINEZERO [7,8]. The paper is organized as follows. The next section focuses on the very moment of the ion ITB triggering and puts in evidence the crucial role of the current profile. In the third section the development of the ITB is addressed. In this phase the ExB shearing is essential for allowing the peaking of the ion temperature. In the fourth section the comparative effects on the linear stability of s and the normalized pressure gradient (α) are studied when the ITB is fully developed. The effect of the reversed current profile on the instabilities spectrum and the behavior of each kind of particles is investigated in section five.

II. ROLE OF THE CURRENT PROFILE IN THE TRIGGERING OF AN ION ITB

In this section we present the linear stability analysis of two shots where the plasma parameters are the same, except for the current profile. These JET discharges are described in [9]. Basically, in the current ramp up phase of the JET shot # 51613, 2 MW of LHCD was applied to form a hollow current profile, then the LH power was switched off before the full power phase (10 MW NBI, 2 MW ICRH). During the application of the full power a wide zone of reduced energy transport clearly occurred at t = 5.7sec., extending from the center out to more than half the plasma radius. On the contrary during the JET shot # 51611 no LHCD was applied and the current profile was monotonic. The other injected powers were virtually the same, however this shot did not develop any ITB. The comparison of these two shots puts clearly in evidence the benefits of the reversed shear profile for the triggering of an ITB. The ion ITBs are widely attributed to the stabilization of the microturbulence caused by the drift wave instabilities, and as far as the current profile is concerned, this stabilization could occur either directly on the linear stability or via an increase of the ExB shearing rate γ_{ExB} whose dependence on the q profile is not simple. We calculated with KINEZERO the radial profile of the maximum electrostatic linear growth rates with low wave numbers ($k_{\perp}\rho_i < 1$) for both shots when the ITB appears in shot 51613 (t=5.7sec.), see fig.1-a . The drift waves concerned are the Ion Temperature Gradient driven mode (ITG) and Trapped Electron Mode (TEM). The shaded regions are the uncertainties due to the error bars on the temperatures and densities profiles. For #51613, in the region of the plasma where the magnetic shear is negative (normalized radius < 0.5), the linear growth rates are significantly lower than for shot #51611. On the contrary, the ExB shearing rates (fig.1b) evaluated with the Hahm-Burrell formula [10] are roughly the same and can not explain the wide barrier. In no way could the increase of the ExB shearing rate be responsible for the triggering of the barrier. Note that in the pre-ITB phase the shafranov shift is roughly the same for both shots at normalized radii > 0.3. Moreover the α

stabilization has been found almost negligible in this region. Thus the main factor is clearly the magnetic shear.

III. GROWTH OF THE ITB

In fig.2 are plotted the radial profiles of the ion temperature at several time slices during (4.2<t<6sec) and after (6<t<13sec) the onset of the ion ITB for the JET shot #53521. This shot presents one of the longest ITB phase ever performed in JET (11sec. electron ITB, 8 sec. ion ITB). During this shot, ITBs were formed and sustained in quasi steady-state condition by combining NBI (15 MW) with RF heating (3 MW of LHCD and 4 MW ICRH) [6]. LH power was applied initially to form a hollow current profile and then to maintain such profile during the high performance phase. In this section we concentrate on the beginning of the ion ITB set up. We have calculated the KINEZERO growth rate at t=4.7, t=4.8 and t=4.9sec, when the ITB is at various states of development. In order to take into account the ExB shearing stabilization we employ the widely used quench rule : Non linear simulations of ITG turbulence [11] have shown that the turbulence suppression arises when $\gamma_{ExB} > k\,\gamma_{lin}^{max}$, where γ_{lin}^{max} is the maximum linear growth rate and k is a factor of order unity. In fig. 3 we plotted altogether these quantities for the three selected time slices. At the beginning (t=4.7sec.) the mixed ITG+TEM modes are completely stable due to the shear reversal, from the center out to 0.3 in norm. radius. The ExB shearing eventually extend this zone of good confinement out to 0.5, but this is not essential to trigger the barrier. As a consequence of the good confinement, the temperature profile is peaking, and the modes are linearly destabilized (t=4.8 and t=4.9sec). However due to the diamagnetic contribution in the radial electrostatic field [12] the ExB shearing rate rises with the pressure second radial derivative, reducing the turbulence which could fully develop otherwise. Thus it is clear that after the triggering by the negative shear stabilization, the ExB shearing becomes essential to allow a full development of the ion ITB.

IV. INVESTIGATION OF S AND STABILIZATION ON ITG+TEM DURING THE FULL ION-ITB PHASE.

It is well known that negative s and high α stabilize the microturbulence by way of the same fundamental mechanism : the reversal of the precession drift of the barely trapped particles and the decrease of the toroidal coupling of passing particles. However it is interesting to study the relative importance of each stabilization in a experimental case. Before the ion-ITB the Shafranov shift stabilization is almost negligible due to low value of α. This is no more the case when the ITB is fully developed, especially when the current profile is deeply reversed, due to the q^2 dependence of α. Even if the α stabilization can not drive the transition into the good confinement state (cf. III.), we have investigated the respective role of s and α in the holding of the ITB. Fig.4 shows the radial profiles of s, q, and α for the JET shot 53521 at t=8sec when the ITB is fully developed, using the CRONOS code in an interpretative way to construct the current profile q [6]. As expected α reaches large values in the core of the discharge (up to 3). In fig.5 we plotted the linear growth rate calculated

in various configurations. First the "real" configuration where α and s are given in fig.4. This curve (full line) shows a strong stabilization at normalized radius $x < 0.4$. This zone corresponds to the negative values of s as well as the large values of α ($\alpha > 1$). The comparison with the curve obtained by artificially setting $\alpha = 0$ (dashed line) puts in evidence the large stabilizing effect of α in a wide region $0.25 < x < 0.5$. Repeating the exercise but setting now α to the experimental value and s to a positive value ($s = +0.5$, dash-dotted line), we see that the stabilizing effect is almost the same as before. Thus in this discharge when the ion-ITB is fully developed both negative shear and large α values are expected to have a significant effect on the stability. However it is worth noting that the negative s values are obtained by LHCD early in the discharge whereas the large α is a consequence of the development of the ion-ITB and could not act as a trigger of the ITB. Finally, it appears that the critical factor is the deeply reversed q profile, as it allows simultaneously large values of α and negative values of s. As an illustration of the global role of the reversed q profile, we have plotted in fig.5 the growth rate obtained with a virtual monotonic q profile as input of the code (dotted line). The monotonic profile has a parabolic dependence upon x, with $q = 1$ at the center of the plasma and $q = 3$ at $x = 0.6$. Due to such a profile both the large α and negative s stabilizing effects are lost, leading to the most unstable case in the core of the discharge.

V. EFFECT OF THE Q PROFILE ON THE MICROTURBULENCE SPECTRUM

Switching to a spectral approach, we plotted in fig.6 the growth rate against the toroidal wave number for JET shot #53521 at $t = 8$ sec and $x = 0.37$ (a). Two peaks, at large and low wave number are separated by a wide gap. By opposition in the case of a monotonic q profile (b) the spectrum is continuous and the growth rates are larger by about one order of magnitude. In addition we have evaluated the mean driving power transferred from each kind of particle to the most unstable mode (fig.7) [13]. A positive value is obtained for destabilizing particles and vice versa. In (b) case the low and very high wave number regions are driven essentially by respectively the passing ions and passing electrons, and trapped electrons dominate the medium wave number range. Conversely in (a) case only the trapped particles destabilize the mode whereas the passing ions are stabilizing and passing electrons have an adiabatic behavior.

REFERENCES

[1]. G.T. Hoang et al., Phys. Rev. Letters, 84 (2000) 4593

[2]. F.M. Levinton et al., Phys. Rev. Letters, 75 (1995) 4417

[3]. E.J. Strait et al., Phys. Rev. Letters, 75 (1995) 4421

[4]. S. Ishida et al., Phys. Rev. Letters, 79 (1997) 3917

[5]. C.D. Challis et al., accepted in Plasma Phys. and Contr. Fusion

[6]. X. Litaudon et al., accepted in Plasma Phys. and Contr Fusion

[7]. C. Bourdelle et al., Contr. Fusion and Plasma Phys. 24B (Proc. 27th EPS conf., 2000) 1092

[8]. C. Bourdelle et al., to be published in nuclear Fusion (may 2002)

[9]. L.G. Eriksson et al., Phys. Rev. Letters, 88 (2002) 145001
[10]. T.S. Hahm and K.H. Burrell, Phys. Plasmas 2 (1995) 1648
[11]. R.E. Waltz et al., Phys. Plasmas 4 (1997) 2482
[12]. K.H. Burrell, Phys. Plasmas 4 (1997) 1499
[13]. C. Fourment et al., to be submitted in Phys. Plasmas

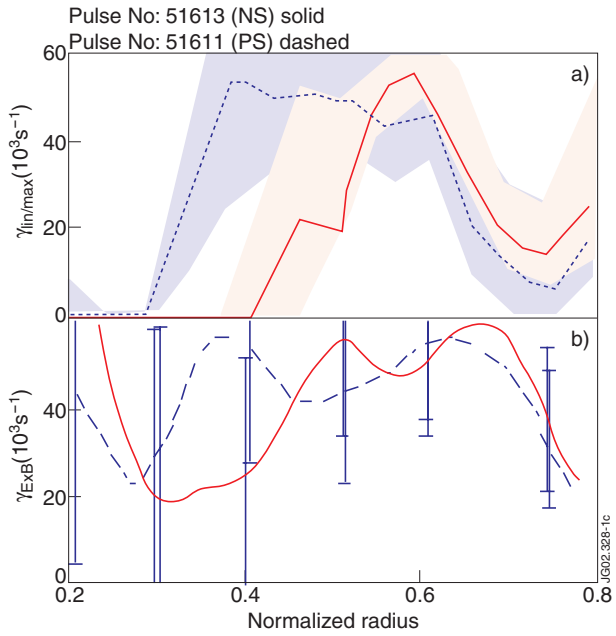

Fig.1 : Radial profiles of simulated linear growth rate (a) and ExB shearing rate (b) for shots #51613 and #51611 at t=5.7 sec.

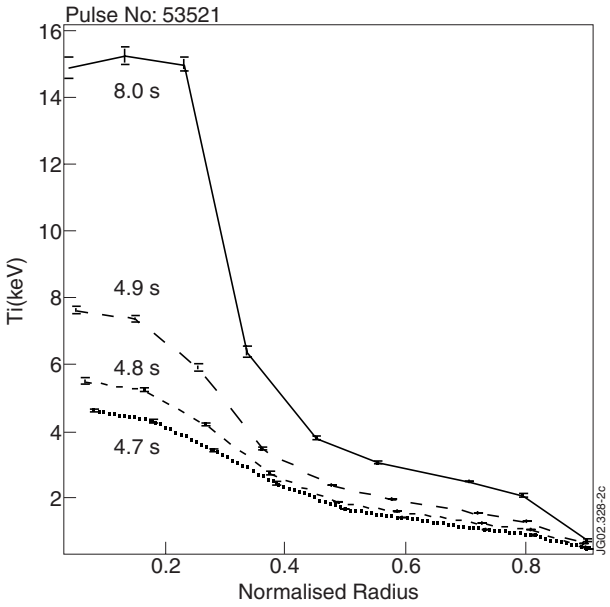

Fig.2 : Radial profile of the ion temperature at various time during and after the ion ITB onset.

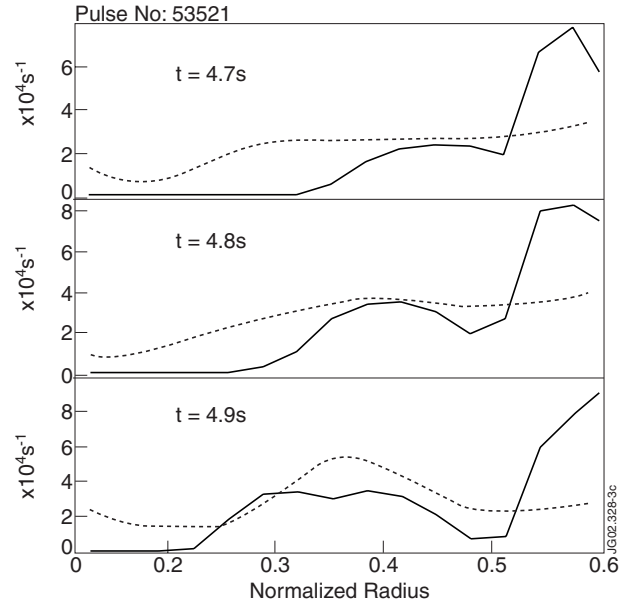

Fig.3 : Radial profiles of the linear growth rate ($k_\perp \rho_i$ <1, full line) and ExB shearing rate (dashed line) during the ITB formation.

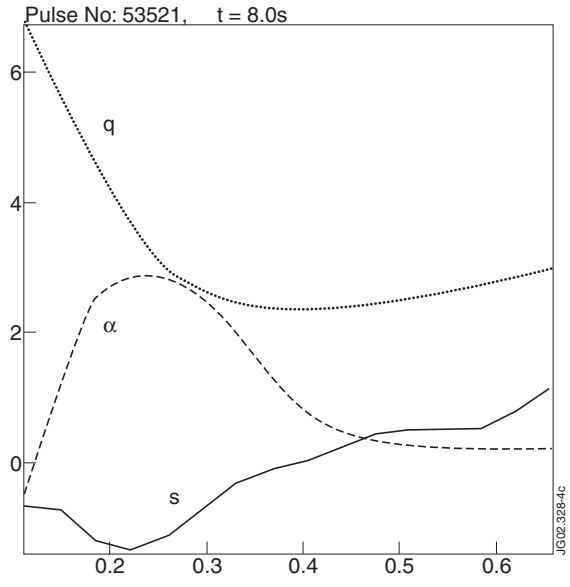

Fig.4 : Radial profile of s, q and α

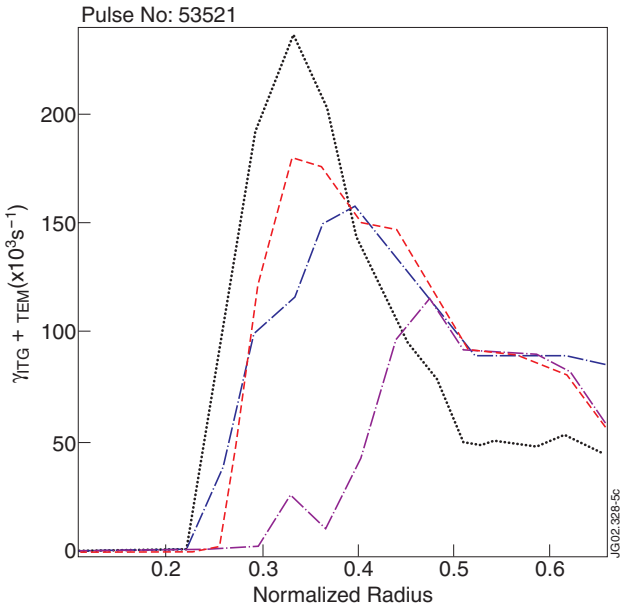

Fig.5 : Radial profile of the maximum ($k_\perp \rho_i$ <1). Full : s and α consistent with CRONOS simulation of fig.4; dashed : α = 0; dash-dot : s = +0.5; dot : s and α consistent with a monotonic q profile

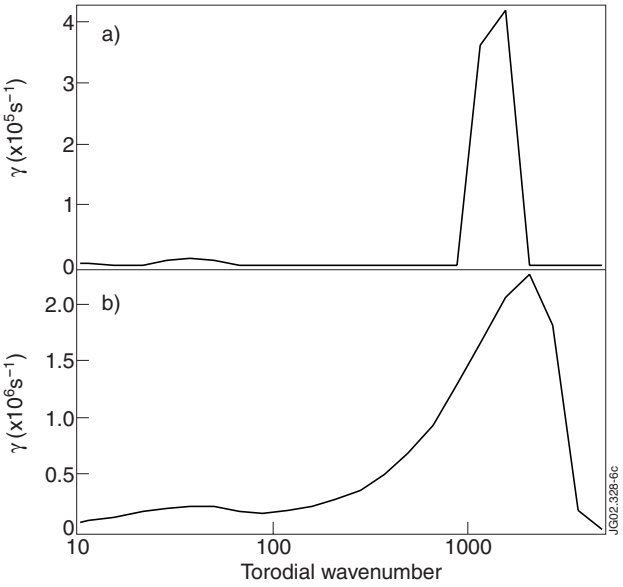

Fig.6 : Growth rate for reversed q profile of fig.4 (a) and monotonic q profile (b) computed at x=0.37

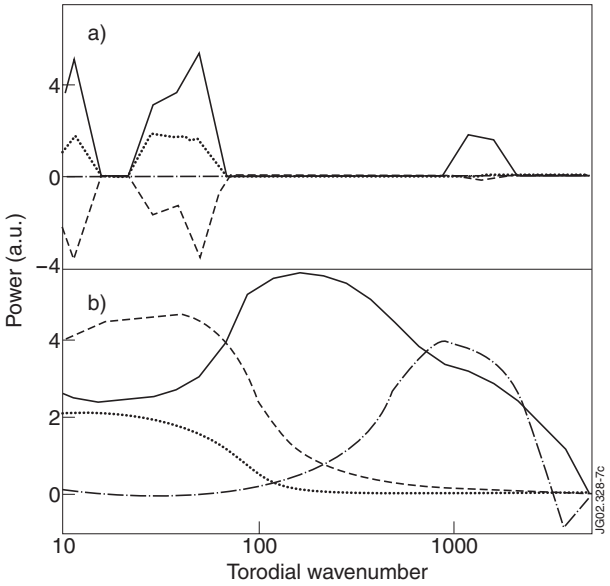

Fig.7 : Mean normalized driving power of each kind of particle. Full : trapped electrons, dashed : passing ions, dots : trapped ions, dashed dot : passing electrons. Same conditions as in fig.6